Appendix A1

Additional information on the parameterization process of the FORMIND forest model including management module and detailed lists of the parameter values used are documented below. Please, find a detailed model description in Fischer et al. (2016) or on the homepage www.FORMIND.org.

A1.1 The model's parameterization

The model landscape is defined as squared area from 1 ha up to several km^2 (in this study 16 ha) being composed of such squared patches (Fig. A1.1.1).

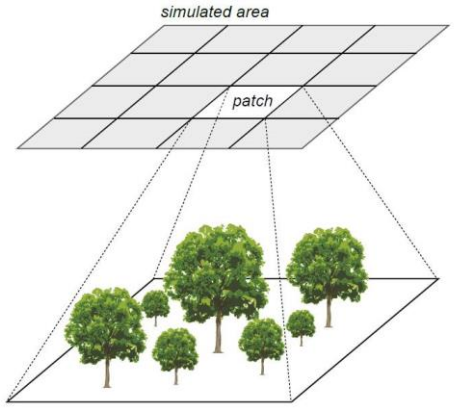

Fig A1.1.1: The FORMIND model's patch structure. The model landscape is defined as squared area from 1 ha up to several km^2 (in this study 16 ha) being composed of squared patches (20 m x 20 m). Patches obtain an explicit spatial position, while the trees within a patch are positioned explicitly depending on the light climate on the ground.

Allometric relations of the trees were modeled on a tree-level for all stem diameter measurements. Undetermined tree species were gathered and their parameter values were averaged. Since wood density is related to the forest stand dynamics, we assigned all available wood densities after Chave et al. (2009) and Zanne et al. (2009) to the tree species and completed undetermined ones by deriving mean wood densities that were genre-, family- or study site-specific. All derived geometric relations were then aggregated group-specifically to model tree growth individually. The functional relations used are documented in Tab. A1.1.1 and the parameter values can be found in Tab. A1.1.2. Throughout the study corrected values of *dbh*-measurements were used (cf. Appendix A1.2).

Tab. A1.1.1: Functional relations used in this study with *agb*: aboveground biomass; *cd*: crown diameter; *circ*: stem circumference; *cl*: crown length; *dbh*: stem diameter at breast height; *dinc*: stem diameter increment; *f*: form factor; *h*: growth height; *lai*: leaf area index; *m*: stem based mortality rate; ρ: wood density; *tr*: fraction of stem biomass to total aboveground biomass. Further basic functions are listed in Fischer et al. (2016).

geometric relation	function
stem circumference-dbh	$dbh(circ) = circ/\pi$
aboveground biomass-dbh	$agb(dbh) = \pi/4 * \rho/tr * dbh^2 * h * f$

crown diameter-dbh	$cd(dbh) = cd_0 * dbh^{cd_1}$
crown length-height	$cl(h) = cl_0 * h$
stem diameter increment-dbh	$dinc(dbh) = a_0 * dbh * (1 - dbh/dbh_{max}) * exp(-a_1 * dbh)$
form factor-dbh	$f(dbh) = f_0 * dbh^{f_1}$
tree height-dbh	$h(dbh) = h_0 * dbh/(h_1 + dbh)$
leaf area index-dbh	$lai(dbh) = l_0 * dbh^{l_1}$
mortality-dbh	$m(dbh) = m_0 * e^{-m_1 * dbh}$

Tab. A1.1.2: *PFT*-specific parameter values and their meaning or unit of the forest model FORMIND used for the Paracou test site.

parameter	description	unit	PFT 1	PFT 2	PFT 3	PFT 4	PFT 5	PFT 6	PFT 7	PFT 8	reference
light and establishment											
k	light extinction coefficient	-	0.7	0.7	0.7	0.7	0.7	0.7	0.7	0.7	Köhler et al. (2003)
n_{seed}	global number of seeds	1 ha^{-1}	2	27	2	15	14	16	20	2	fine-tuned
i_{seed}	min. light intensity to establish	-	0.01	0.01	0.05	0.20	0.01	0.02	0.15	0.01	Köhler et al. (2003)
geometry											
h_{max}	max. growth height	m	16.50	34.22	34.61	34.85	40.40	39.96	38.58	39.06	derived from inventory data
h_0	height-dbh-relation	-	47.0	47.0	47.0	47.0	47.0	47.0	47.0	47.0	calculated from Molto, Hérault, Boreux, et al. (2014b); Molto, Hérault, Boreux, et al. (2014a)
h_1	height-dbh-relation	-	0.276	0.276	0.276	0.276	0.276	0.276	0.276	0.276	calculated from Molto, Hérault, Boreux, et

											al. (2014b); Molto, Hérault, Boreux, et al. (2014a)
cd_0	crown diameter-dbh-relation	-	13.12	13.12	13.12	13.12	13.12	13.12	13.12	13.12	calculated from Jucker et al. (2017)
cd_1	crown diameter-dbh-relation	-	0.59	0.59	0.59	0.59	0.59	0.59	0.59	0.59	calculated from Jucker et al. (2017)
l_0	lai-dbh-relation	-	2.0	2.0	2.0	2.0	2.0	2.0	2.0	2.0	Köhler et al. (2003)
l_1	lai-dbh-relation	-	0.0	0.0	0.0	0.0	0.0	0.0	0.0	0.0	Köhler et al. (2003)
f_0	form factor-dbh-relation	-	0.425	0.425	0.425	0.425	0.425	0.425	0.425	0.425	derived from inventory data
f_1	form factor-dbh-relation	-	-0.18	-0.18	-0.18	-0.18	-0.18	-0.18	-0.18	-0.18	Fischer et al. (2014)
cl_0	crown length factor-height-relation	-	0.358	0.358	0.358	0.358	0.358	0.358	0.358	0.358	Köhler et al. (2003)
σ	fraction of stem biomass-total biomass	-	0.7	0.7	0.7	0.7	0.7	0.7	0.7	0.7	derived from inventory data
biomass and productivity											
ρ	wood density	$t * m^{-1}$	0.76	0.77	0.66	0.55	0.83	0.73	0.56	0.62	calculated from Chave et al. (2009);Zanne et al. (2009)
M	transmission coefficient	-	0.1	0.1	0.1	0.1	0.1	0.1	0.1	0.1	Larcher (1994)

	of leafs										
G	gross productivity to respiratory costs	-	0.2	0.2	0.2	0.2	0.2	0.2	0.2	0.2	Rico fragen nach Quelle
α	slope of light response curve	$\mu mol_{CO_2} * \mu mol_{photo}^{-1}$	0.043	0.043	0.035	0.086	0.043	0.043	0.086	0.043	Köhler et al. (2003)
p_{max}	maximum leaf photosynthesis	$\mu mol_{CO_2} * (m^2 * s)^{-1}$	1.12	0.55	2.00	20.59	1.35	1.50	27.00	1.46	fine-tuned
g_{max}	maximum annual stem diameter increment	m/yr	0.011	0.018	0.017	0.014	0.025	0.013	0.022	0.031	derived from inventory data, fine-tuned
g_{dbhmax}	maximum stem diameter	-	0.24	0.17	0.12	0.11	0.30	0.11	0.17	0.37	derived from inventory data, fine-tuned
mortality											
m_{mean}	background mortality rate	-	0.01	0.01	0.013	0.02	0.01	0.01	0.02	0.01	derived from inventory data
fallP	probability of dead tree to fall	-	0.5	0.5	0.5	0.5	0.5	0.5	0.5	0.5	derived from inventory data
management module											
$comm_{spec}$	proportion of commercially logged species	-	0.0	0.0362	0.2393	0.0865	0.5718	0.5531	0.3311	0.2706	derived from inventory data
log_{dbh}	cutting threshold of mean stem diameter	[m]	0.55	0.55	0.55	0.55	0.55	0.55	0.55	0.55	derived from inventory data

Calibration, and fine tuning. The parameters describing the photosynthesis (p_{max}), the slope of the light response curve (α), the maximum stem diameter growth rates (g_{max}, g_{dbhmax}), and the number of seeds

(N_{seed}) are important for the succession of the forest stand and the composition of the tree species. These parameters were numerically calibrated and fine-tuned using the dynamically dimensioned search *DDS* (Lehmann and Huth 2015). The simulation results of the model (aboveground biomass, stem number, basal area) were calibrated using aggregated criteria derived from Paracou's forest inventory data of the T0-control plots (Fig. A1.2.1). The Paracou data represent a forest at its equilibrium state. The *DDS* method ran with $1.0 * 10^6$ iterations and a search radius of 0.2. The cost function computed the standard error *Q* between the observed *o* and modeled *m* values as follows:

$$Q = Q_B + Q_N = \sum_p (\omega_{Bp} * |Q_{Bp}|) + \sum_p (\sum_d (\omega_{Dd} * |Q_{Nd}|) * \omega_{Bp})$$
$$= \sum_p (B_{op}/B_{ot} * |(B_{mp} - B_{op})/B_{op}| + \sum_p (\sum_d (D_d/D_t * |(N_{md} - N_{od})/N_{od}|) * B_{op}/B_{ot})$$

with Q_B and Q_N as weighted relative errors and the indices representing the aboveground biomass *B* and stem numbers *N*. Q_B and Q_N equal the sums over all absolute values of their relative errors multiplied with weighing factors ω. The relative errors between the observed *o* and modeled *m* values of *B* or *N* were calculated either for each plant functional type *p* or each stem diameter class *d* (class width = 0.1 m). The weights ω_{Bp} and ω_{Dd} were determined regarding either the *PFT*'s observed aboveground biomasses or the mean stem numbers *D* per stem diameter class *d* as fraction of their total sums *t*. The weighting of the *PFT*'s aboveground biomasses and the stem numbers should ensure that the model output, necessary for answering the research questions, was modeled precisely. Decisive for the quality of the cost function were the appropriateness of the weighting factorsω. This led to the fact that the aboveground biomass of more dominant *PFT*s and the frequency of tall trees with a large stem diameter had a greater impact on the simulation result during the parameter set's fine-tuning. Ranges of the fine-tuned parameters are shown in Tab. A1.1.3.

Tab. A1.1.3: Model calibration and fine-tuning. *PFT*-specific ranges of the parameter values that were fine-tuned using the dynamically dimensioned search *DDS* (Lehmann and Huth 2015).

pft	range of n_{seed}	range of p_{max}
1	[1; 10]	[0.9; 3.0]
2	[1; 35]	[0.4; 3.0]
3	[1; 60]	[3.0; 10.0]
4	[15; 100]	[10.0; 25.0]
5	[1; 25]	[0.9; 3.0]
6	[1; 60]	[3.0; 10.0]
7	[15; 100]	[10.0; 28.0]
8	[1; 25]	[0.9; 3.0]

The values for p_{max} and n_{seed} are based on knowledge from previous studies (e.g. (Hiltner et al. 2016; Fischer et al. 2016; Fischer et al. 2014; Köhler et al. 2003)). It was important that the calibrated parameters did not reach the upper or lower limits. All parameter values used in the parameterization of the FORMIND forest model are documented in Table A1.1.2.

Due to this approach, the forest model of FORMIND was calibrated against 136 data points originating from the forest inventories: taking eight *PFT*s by stem numbers of 16 stem diameter classes and their

aboveground biomass of the cost function. Extensive preliminary testing of cost functions showed that the chosen criteria were the most effective within this study. Fig. A1.1.2 shows the results of the fine-tuning by presenting the total forest stand's tree size distribution. For trees with a *dbh* smaller than 0.4 m, the number of trees was slightly overestimated by the model, whereas the number of larger trees was very well recorded.

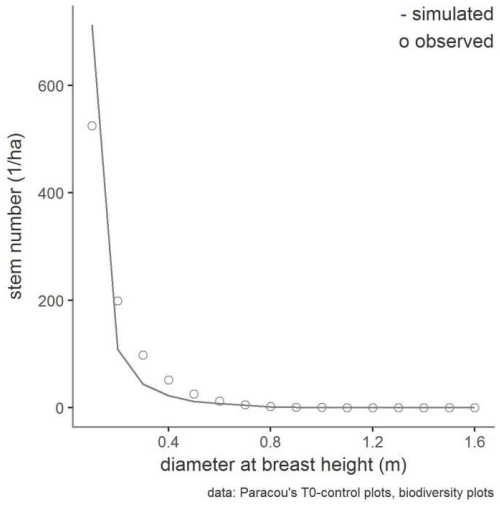

Fig A1.1.2: Model calibration. Comparison of the simulated and observed mean root number tree size distribution of the entire forest stand. The mean values of the observations were calculated from the forest inventory data of the T0 control areas and biodiversity areas (cf. A1.2.1) of the period 1984-2016. The simulated mean values were averaged over 16 ha and over the years 333-1000, assuming that the forest was in equilibrium of a mature forest.

Results of model calibration

Kommentar [UH1]:
Diskussionspunkt: Da das Manuskript bereits länger ist, könnte man darüber nachdenken, die Modelkalibrierung und den Vergleich mit den Felddaten in den Anhang zu verschieben – damit hätte man den Fokus ausschließlich auf dem Logging.

The first research question was answered: The forest model mapped the structure of the undisturbed growth dynamics of the forest. This applies to a mature forest stand in the equilibrium phase at the test site of Paracou. The forest model was able to describe both the structure of the stand, i. e. the tree species composition and tree size distribution, as well as the growth dynamics, i. e. the succession, over the simulated period of time. In order to obtain this result, the distributions of the *PFT*-specific mean attribute values of the aboveground biomass, basal area of each functional species group *pft* were taken into account during manual calibration. Subsequently, in automated fine-tuning with the *DDS* method (Lehmann and Huth 2015), the deviations between simulated and observed distribution of the number of stems per trunk diameter class (class width: 0.1 m) were minimized. The choice of the appropriate cost function played an important role (Appendix A1).

Fig. 3.1 shows the calibration results for the aboveground biomass *agb* and basal area *ba*. It can be seen that both the observed and simulated attribute values are affected by a certain variability represented by the standard deviation *sd*. The reason for this is that the data basis was subject to stochasticity, which is inherent in the natural dynamics of growth processes. Firstly, we compared the observed and simulated attribute values of the aboveground biomass over time in order to evaluate the succession dynamics of the individual species groups (Fig. 3.1.a). Only simulation results of the equilibrium phase of the forest stand were taken into account (simulated time > 333 a). The simulated succession of the aboveground biomass

per *PFT* was consistent. At the beginning of the simulation time, the fast-growing pioneer species and, most recently, the slow-growing climate species first established themselves on the treeless area; the intermediary *PFT*s followed in between. Secondly, we compared the simulated and observed mean basal area (Fig. 3.1.b). In this case, it was optimal if attribute value pairs were exactly on the bisectors of the angle. This defined optimum was difficult to achieve during model calibration due to non-linear relationships between model processes. For this reason, tolerance limits were allowed within which the model had to reproduce reality with sufficient accuracy. This tolerance limit was defined as follows: The simulated attribute values should be within the range of the observed variability sd_{obs}. The observed standard deviation of the attributes was therefore projected on the simulation results ($sd_{sim} = sd_{obs}$). This resulted in the grey confidence range for the attribute value of the total stand. To show the reliability of all *PFT*-specific attribute values, this confidence range was projected by centric stretching as a percentage of the origin. Our forest model of the Paracou site overestimated the total mean of observed aboveground biomass (418.0 t_{ODM}/ha) slightly by 5% and the total mean of the observed basal area (30.72 m^2/ha) by 9%. The deviations between observed and simulated attributes of the *PFT*s of both the aboveground biomass and the basal area were less than the sd_{obs}. Only the PFT3 and PFT7 exceeded the tolerance limits of the projected standard deviation. Since both *PFT*s had low attribute values, their overestimation was hardly noticeable at the entire stand level. The calibrated forest model served as a basis for the validation of the management module. Additionally, the differences in variance between the simulated and observed attribute values of each *PFT* were very small, for both aboveground biomass (R^2 0.99444, rmse 4.65934) and the basal area (R^2 0.99416, rmse 0.33322).

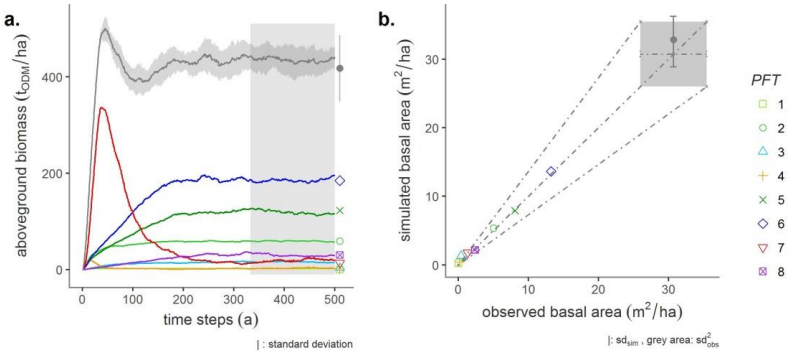

Fig 3.1: Calibration results. Comparison between the observed (dots) and simulated (line graphs) aboveground biomass development (a.) as well as the mean basal area (b.) for each plant functional type *PFT* and the total stand. Light-demanding pioneers are reddish, shade-tolerant climate species are greenish, emergent are violet, and intermediate species are bluish-colored. During model calibration, only simulation results of the years 333-1000 were taken into account. The simulated attribute values were within the range of the observed variability sd_{obs}. Observed standard deviation of the attributes was then projected on the simulation results (grey area).

Results of model validation: quantification of damage by selective logging

Decisive for the model validation was to objectively check whether the usage target had been achieved. Furthermore, model validation and verification should be successful independently of each other. Therefore, different inventory data sets from the verification were used for the validation test (T1 logging plots; cp. chap. 2.2). The aim of the validation of the Paracou model was to answer our second research question: Is the calibrated forest model with the added management module able to represent the structure

and dynamics of a selectively logged forest stand? The calibrated forest model served as a basis for the validation of the management module. The damage to the forest stand was defined as model parameter dam_l. The values were calculated from forest inventory data of the T1-*RIL* plots of the Paracou test site, depending on the *dbh*-classes dam_{dia}. The number of commercial tree species harvested and the loss of mean annual aboveground biomass were investigated as simulation results.

Fig. 3.2.a shows the temporal development of the aboveground biomass as a secondary succession after 1986. In order to make the time series (observed vs. simulated) comparable, the simulated disturbance event was assigned to the year of the observed disturbance event in 1986. Between 1986 and 2016, the difference between simulated and observed annual mean values of aboveground biomass per *PFT* should be less than the standard deviations *sd* of the observed attribute values. In the period under consideration (1987-2016), the variance of the simulated aboveground biomass deviated only little from the observed attribute values (R^2 0.99084, rmse 4.63054). Only for PFT5, the model slightly underestimated biomass in the first years after selective logging until the year 2000. In contrast to the observed attribute values of PFT7 and PFT3 (fast-growing pioneer species), the simulated biomass shows a very short but significant peak (1987-1989). Simulated and observed curves stabilize themselves immediately afterwards.

Furthermore, the model of the Paracou test site estimated the exact number of trees harvested from all commercial tree species. During logging in 1986, around 33.0 t_{ODM}/ha of aboveground biomass or 10 trees per hectare were harvested on the T1-*RIL* plots in Paracou. With the simulated harvest of 10 commercially usable trees per hectare and a loss of 33.0 t_{ODM} biomass per hectare, the model provided a very good estimation of the damage and harvest. In particular, the model reacted sensitively to the parameter dam_l. In Fig. 3.2.b it is shown that the rate of damage to the remnant forest stand determined from forest inventory data decreases with increasing *dbh*.

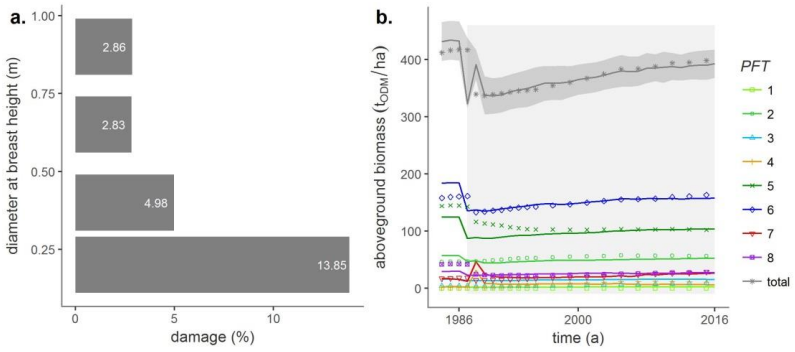

Fig 4.1: Validation results. a.) The damage to the forest stand of the Paracou test site by man and machine was defined as model parameters, and the values were calculated as a function of four log diameter classes based on forest inventory data of the T1-*RIL* plots. b.) Comparison of the temporal development of observed (dots) and simulated (line graph) aboveground biomass after the selective logging event in 1986 (grey area). Light-demanding pioneers are reddish, shade-tolerant climate species are greenish, emergent are violet, and intermediate species are bluish-colored.

The simulation experiment was intended to investigate damages of selective logging on forest growth conditions. Fig. A1.1.3 shows the development of aboveground biomass for the simulation experiment group-specifically.

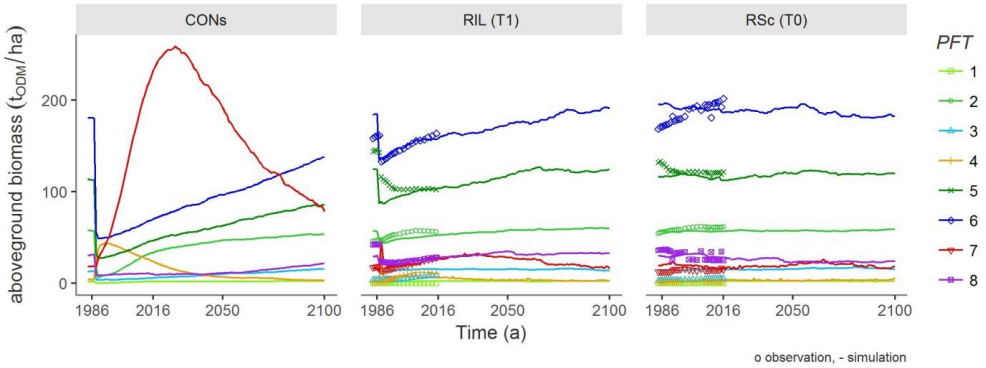

Fig. A1.1.3: Simulation results of all scenarios on *PFT*-level. Points represent observed mean aboveground biomass calculated from forest inventory data regarding different successional stages. Time series represent mean *agb* and *sn* of simulation results starting from bare ground per hectare with standard deviations of 10 ha.

3.1. Model calibration

The first research question was answered: The forest model mapped the structure of the undisturbed growth dynamics of the forest. This applies to a mature forest stand in the equilibrium phase at the test site of Paracou. The forest model was able to describe both the structure of the stand, i. e. the tree species composition and tree size distribution, as well as the growth dynamics, i. e. the succession, over the simulated period of time. In order to obtain this result, the distributions of the *PFT*-specific mean attribute values of the aboveground biomass, basal area of each functional species group *pft* were taken into account during manual calibration. Subsequently, in automated fine-tuning with the *DDS* method (Lehmann and Huth 2015), the deviations between simulated and observed distribution of the number of stems per trunk diameter class (class width: 0.1 m) were minimized. The choice of the appropriate cost function played an important role (Appendix A1).

Fig. 3.1 shows the calibration results for the aboveground biomass *agb* and basal area *ba*. It can be seen that both the observed and simulated attribute values are affected by a certain variability represented by the standard deviation *sd*. The reason for this is that the data basis was subject to stochasticity, which is inherent in the natural dynamics of growth processes. Firstly, we compared the observed and simulated attribute values of the aboveground biomass over time in order to evaluate the succession dynamics of the individual species groups (Fig. 3.1.a). Only simulation results of the equilibrium phase of the forest stand were taken into account (simulated time > 333 a). The simulated succession of the aboveground biomass per *PFT* was consistent. At the beginning of the simulation time, the fast-growing

pioneer species and, most recently, the slow-growing climate species first established themselves on the treeless area; the intermediary *PFT*s followed in between. Secondly, we compared the simulated and observed mean basal area (Fig. 3.1.b). In this case, it was optimal if attribute value pairs were exactly on the bisectors of the angle. This defined optimum was difficult to achieve during model calibration due to non-linear relationships between model processes. For this reason, tolerance limits were allowed within which the model had to reproduce reality with sufficient accuracy. This tolerance limit was defined as follows: The simulated attribute values should be within the range of the observed variability sd_{obs}. The observed standard deviation of the attributes was therefore projected on the simulation results ($\boldsymbol{sd_{sim} = sd_{obs}}$). This resulted in the grey confidence range for the attribute value of the total stand. To show the reliability of all *PFT*-specific attribute values, this confidence range was projected by centric stretching as a percentage of the origin. Our forest model of the Paracou site overestimated the total mean of observed aboveground biomass (418.0 t_{ODM}/ha) slightly by 5% and the total mean of the observed basal area (30.72 m^2/ha) by 9%. The deviations between observed and simulated attributes of the *PFT*s of both the aboveground biomass and the basal area were less than the sd_{obs}. Only the PFT3 and PFT7 exceeded the tolerance limits of the projected standard deviation. Since both *PFT*s had low attribute values, their overestimation was hardly noticeable at the entire stand level. The calibrated forest model served as a basis for the validation of the management module.Additionally, the differences in variance between the simulated and observed attribute values of each *PFT* were very small, for both aboveground biomass (R^2 0.99444, rmse 4.65934) and the basal area (R^2 0.99416, rmse 0.33322).

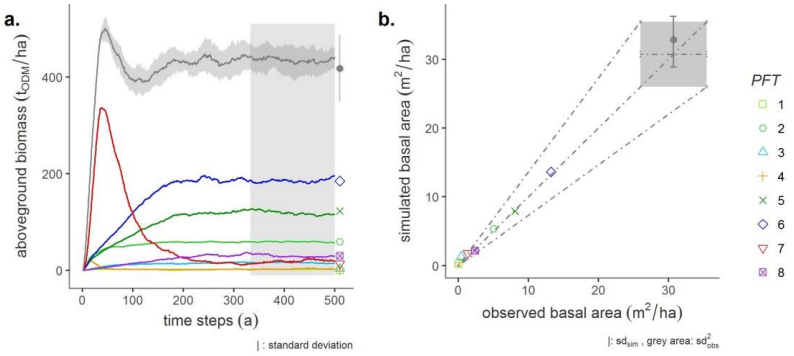

Fig 3.1: Calibration results. Comparison between the observed (dots) and simulated (line graphs) aboveground biomass development (a.) as well as the mean basal area (b.) for each plant functional type *PFT* and the total stand. Light-demanding pioneers are reddish, shade-tolerant climate species are greenish, emergent are violet, and intermediate species are bluish-colored. During model calibration, only simulation results of the years 333-1000 were taken into account. The simulated attribute values were within the range of the observed variability sd_{obs}. Observed standard deviation of the attributes was then projected on the simulation results (grey area).

3.2 Model validation: quantification of damage by selective logging

Decisive for the model validation was to objectively check whether the usage target had been achieved. Furthermore, model validation and verification should be successful independently of each other. Therefore, different inventory data sets from the verification were used for the validation test (T1 logging plots; cp. chap. 2.2). The aim of the validation of the Paracou model was to answer our second research question: Is the calibrated forest model with the added management module able to represent

the structure and dynamics of a selectively logged forest stand? The calibrated forest model served as a basis for the validation of the management module. The damage to the forest stand was defined as model parameter dam_l. The values were calculated from forest inventory data of the T1-*RIL* plots of the Paracou test site, depending on the *dbh* classes dam_{dia}. The number of commercial tree species harvested and the loss of mean annual aboveground biomass were investigated as simulation results.

Fig. 3.2.a shows the temporal development of the aboveground biomass as a secondary succession after 1986. In order to make the time series (observed vs. simulated) comparable, the simulated disturbance event was assigned to the year of the observed disturbance event in 1986. Between 1986 and 2016, the difference between simulated and observed annual mean values of aboveground biomass per *PFT* should be less than the standard deviations *sd* of the observed attribute values. In the period under consideration (1987-2016), the variance of the simulated aboveground biomass deviated only little from the observed attribute values (R^2 0.99084, rmse 4.63054). Only for PFT5, the model slightly underestimated biomass in the first years after selective logging until the year 2000. In contrast to the observed attribute values of PFT7 and PFT3 (fast-growing pioneer species), the simulated biomass shows a very short but significant peak (1987-1989). Simulated and observed curves stabilize themselves immediately afterwards.

Furthermore, the model of the Paracou test site estimated the exact number of trees harvested from all commercial tree species. During logging in 1986, around 33.0 t_{ODM}/ha of aboveground biomass or 10 trees per hectare were harvested on the T1-*RIL* plots in Paracou. With the simulated harvest of 10 commercially usable trees per hectare and a loss of 33.0 t_{ODM} biomass per hectare, the model provided a very good estimation of the damage and harvest. In particular, the model reacted sensitively to the parameter dam_l. In Fig. 3.2.b it is shown that the rate of damage to the remnant forest stand determined from forest inventory data decreases with increasing *dbh*.

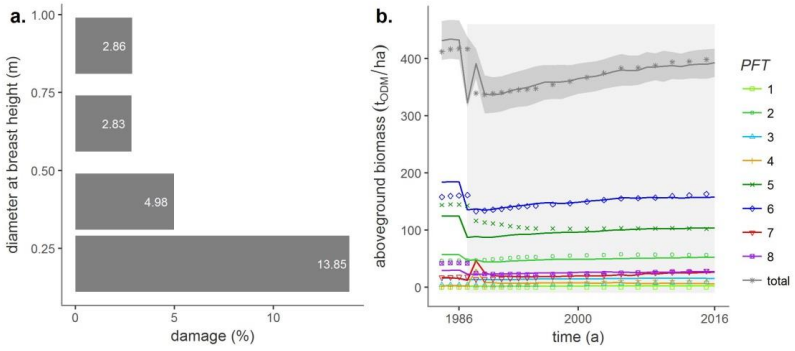

Fig 4.1: Validation results. a.) The damage to the forest stand of the Paracou test site by man and machine was defined as model parameters, and the values were calculated as a function of four log diameter classes based on forest inventory data of the T1-*RIL* plots. b.) Comparison of the temporal development of observed (dots) and simulated (line graph) aboveground biomass after the selective logging event in 1986 (grey area). Light-demanding pioneers are reddish, shade-tolerant climate species are greenish, emergents are violet, and intermediate species are bluish-colored.

3.3. Simulation experiment: Changes in biomass and production after damage by selective logging

The basis for the simulation experiment of this study to investigate different damages caused by selective logging was the validated forest model including the management module of the Paracou test site. Through model validation, the reliability of the model became known. The third research question was answered with the help of three simulation scenarios: How resilient is the forest stand until the end of the 21st century? The simulated logging event was assigned to the observed event in 1986 and the entire simulation period considered was between 1984 and 2100 (Fig. 3.3.a). This means that for the *RSc* scenario (undisturbed growth conditions) and the *RIL*-scenario (*reduced impact logging*), we analyzed the biomass development for a forecast period of more than 95 years. The conventional scenario *CONs*, on the other hand, was a fictitious example for which 3-16 times higher (depending on stem diameter class) damage rates through men and machine were assumed (Fig. 3.3 b).

Fig. 3.3. a shows the results of the simulation experiment of all three scenarios indicating the temporal development of the total aboveground biomass. It can be clearly seen that the 1986 disturbance in both logging scenarios was followed by an immediate decline in aboveground biomass. In comparison to the reference *RSc* in both logging scenarios, the number of trees harvested as well as the harvested stem volume was equal: 10 stems per hectare and 52 m^3/ha stem volume. Due to the different intensities of damage, however, the remaining total aboveground biomass per logging scenario differed considerably. The damaged stand volume of the *RIL* amounted to 33 t_{ODM}/ha. This was more than five times higher in the *CONs* (-179 t_{ODM}/ha). Directly after logging, the development of biomass varied according to the simulation scenario: (*i.*) The secondary succession of the *CONs* scenario was characterized by two periods during the recovery phase (1987-2050). A rapid increase in forest biomass was recorded until after about 30 years the status quo was reached for the first time. A period of increased resilience followed until about 2050, when the maximum stock biomass was reached after about 15 years (2025). In the first half of strengthened resilience, gross primary production was slower but positive. The local maximum of the stand biomass proved to be unstable, so that it fell back to the reference values (433 t_{ODM}/ha) until 2050. Subsequently, it settled to a lower secondary equilibrium level of (399 t_{ODM}/ha) until the end of the simulation period considered, in 2100. (*ii.*) During the approximately 70-year recovery phase, until 2050, the secondary succession of the total aboveground biomass of the *RIL* scenario took place with a smaller but steady gradient, so that after about 70 years (2050) the status quo was reached first time again. In the subsequent equilibrium phase (> 2050), the total aboveground biomass piled up slightly above the reference value at 450 t_{ODM}/ha. A tipping point, followed by a system collapse, did not show any of the simulation scenarios due to the damage investigated.

With regard to the research question three, changes in forest structure should be analyzed in addition to biomass dynamics. This was determined using the simulated species group composition. The results at the PFT level are shown below (Annex A1.1). The tree species composition of the secondary succession of the *RIL* scenario shifted slightly in the 70 years after the logging event: The aboveground biomass of the pioneer species in PFT6 (upper canopy layer) recovered faster than that of the climax tree species in PFT5 and PFT8 until about 2040. In undergrowth, the aboveground biomass of PFT1 remained constant. This group of species was neither used commercially nor influenced by structural variations of the forest stand. The rejuvenation rates of the intermediate species groups belonging to the higher canopy layers

(PFT3 and PFT6) were between pioneer and climax species groups. After 2050, the tree species composition structure of the *RIL* scenario returned to the reference. In contrast to the *RIL* scenario, the species group composition of the *CONs* scenario was heavily shifted. This mainly concerned groups of species, with large trees of the upper two canopy layers (PFT5-PFT8). Neither PFT5 nor PFT8 reached the status quo of the reference before the logging event. Overall, the intermediary tree species of the PFT7 developed at the most dominant during the secondary succession. They grew fastest and exceeded the reference value after only 10 years. This strengthened resilience behavior of PFT7 explained the curve shape of the total biomass in the *CONs* scenario (Fig. 3.3.a).

Figure 3.3.b shows a comparison of the density functions of the gross primary production *ggp* of all three simulation scenarios starting from the moment of the logging event in 1986. While the equilibrium phase, the *gpp* of the *RIL* scenario in was close to the reference and the dispersion was low indicating a stable trend in biomass production. Median values of the scenario-dependent density distributions of both resilience phases enabled an ordinal evaluation of the scenarios. The distribution of *gpp* of the *CONs* scenario was more broadly diversified and the median value was higher than that of the reference. The median does not return to its initial state during the considered period of time. Note that with normally distributed data, the median corresponds to the arithmetic mean.

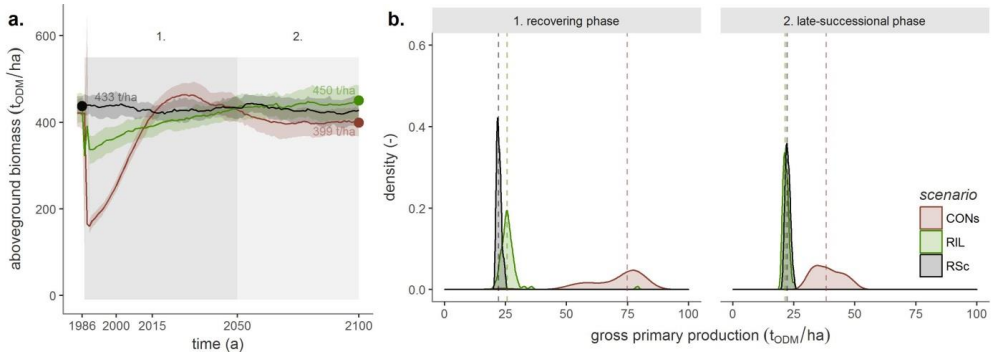

Fig 4.1: Simulation experiment. a.) Results for the scenario settings used in FORMIND, simulated over 116 years for the forest stand of Paracou (line graphs). Starting from an equilibrium phase of the primary succession, the development of the aboveground biomass after a logging event (1986) until the end of the 21st century is presented. The dots indicate the averaged values of the simulation results either for a 50-year spin-up period (primary succession) or secondary succession. b.) Scenario-dependent density distributions of gross primary production after selective logging in 1986, shown for the two phases of secondary succession: recovering phase (1987-2050) and late-successional phase (2051-2100). Median values (dashed lines) enable an ordinal evaluation of the scenarios.

A1.2 The experimental design

The experimental design at the test site is shown schematically in the global map of Paracou (Fig. A1.2.1).

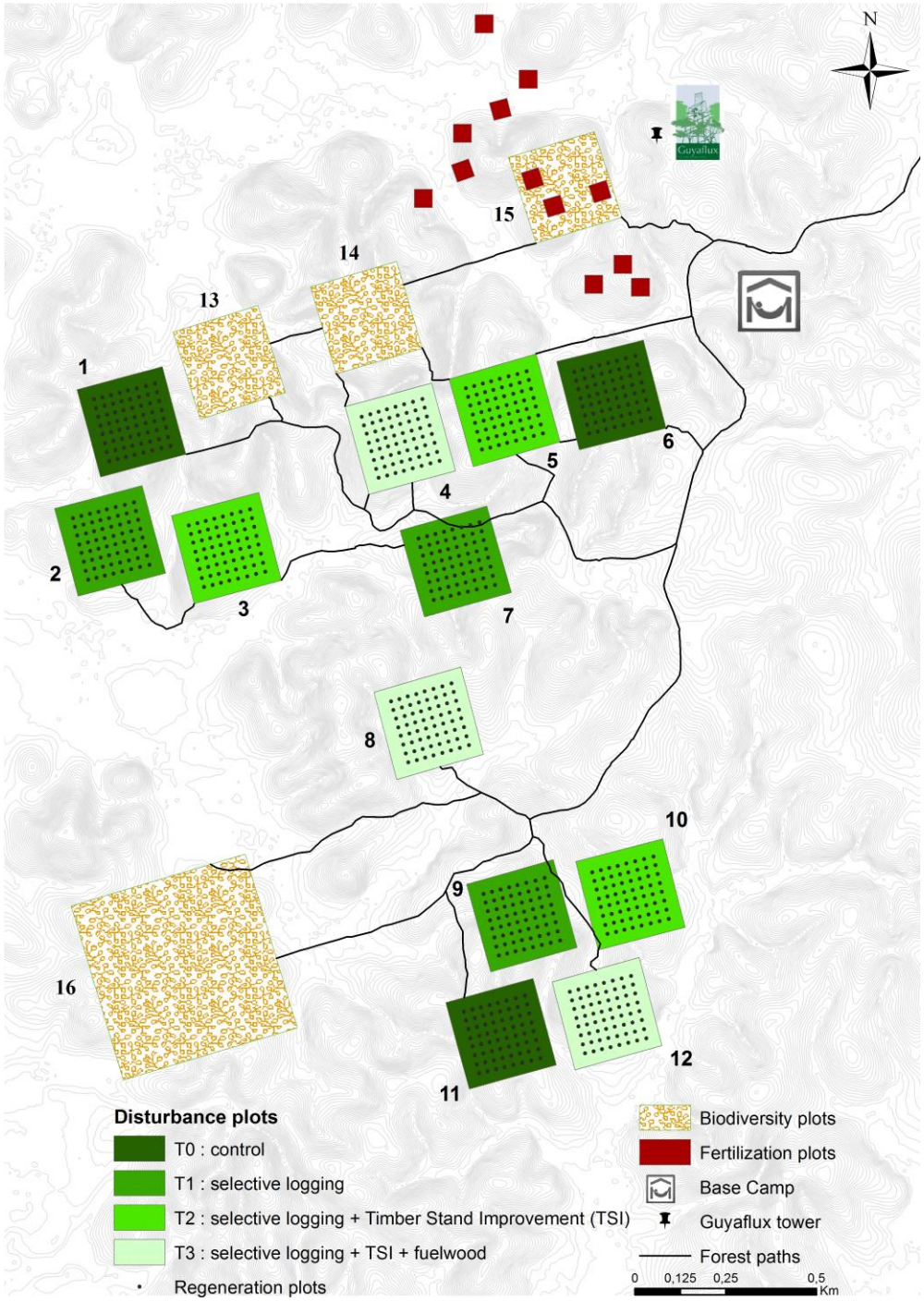

(**???**) Fig A1.2.1: The global map of Paracou's experimental design (CIRAD 2016). To parameterize and

calibrate the forest model of FORMIND we used forest inventory data of the T0-control plots and biodiversity plots. The parameterization and validation of FORMIND's management module is based on forest inventory data of the T1-logging plots.

The correction of *dbh* measurements. In some cases the normal *dbh* measurement was not possible, so that the measuring point was adjusted according to four rules. The type of rule shows tab. A1.2.1. In order to eliminate bias caused by such an adjustment of the measuring points, a correction of the primary circumferential measurement was calculated, which was used in the course of the study.

Tab. A1.2.1: Coding for the measuring point of the trunk circumference [cm] in Paracou's forest inventory data set.

coding	meaning
0	normal measure at 1.3 m
1	elevated measure at 0.5 m
2	elevated measure at 1.0 m
3	elevated measure at 1.5 m
4	tree with irregular stem

The types of damage through logging. It was possible to model logging damages that were defined as the damage to the remaining forest stand. We obtained information about the proportion of damaged trees from the total number of trees, from the inventory data of the T1-*RIL* plots of Paracou (cf. Fig. A1.2.1). Table A1.2.1 shows the coding of damage through logging.

Tab. A1.2.2.: Coding for the type of damage (code_resume) and its meaning in Paracou's forest inventory data set. Code alive indicates whether a tree is still alive or not (1: true, 0: false).

coding alive	coding measure	meaning
0	1	dead tree, destroyed through overthrow of logged trees
0	5	dead tree, destroyed through man and machine
0	8	dead tree, destroyed after exploitation

In FORMIND the parameter dam_1 was calculated as fraction of the sum of counted stems n of dead trees through logging and all trees on the T1-*RIL*-plots n_t, with the indices indicating the type of damage *code alive*|*code measure*:

$$dam\ dia\ = (n_{0|1} + n_{0|5} + n_{0|8})/n_t.$$

Appendix A2

Software used. To process the data of Paracou's forest inventories as well as the simulation results of FORMIND (Fischer et al. 2016), version 3.4.1 of the R statistical software (R Core Team, 2017) with the packages 'tidyverse' v1.1.1 (Wickham, 2017), 'modelr' v0.1.0 (Wickham, 2016), 'splines' (R Core Team, 2017), 'bookdown' v.0.4 (Xie, 2017) were used.

MOOP v0.21 was used (Lehmann and Huth 2015) during the fine-tuning of the FORMIND forest model.